Open-source Testbed for Body Area Networks: 200 sample/sec, 12 hrs Continuous Measurement.

Leif Hanlen[12], Vasanta Chaganti[12], Ben Gilbert[1], David Rodda[1], Tharaka Lamahewa[12], David Smith[12]
[1]National ICT Australia and
[2]College of Engineering and Computer Science, The Australian National University

***Abstract*—We present the design criteria and specifications of a novel Open-Source hardware channel sounder and Open-Source data sets for measurements of the Body Area Channel at the 2400MHz ISM band and 2360MHz band. We outline a need for open hardware and measurement data to facilitate robust standardization of the new Body Area Networks. We demonstrate typical analyses on a public data set, with reference to previous works, and show how complex network topologies may be simulated through simple real measurements using reciprocity.**

I. Introduction

Body area networks (BANs) are attracting interest as the next generation of (personal) wireless networks. The potential for BANs, when combined with smart wireless sensing environments [1] and mass-produced implantables [2] is enormous. The IEEE task group 802.15.6 will form a baseline document, including MAC [3] and narrowband PHY [4] proposals. The 802.15.6 channel model [5] contains several narrowband channel models. Radio models for body area networks have largely neglected complex network, and realistic movement scenarios. There is also a lack of uniformity in measurement campaigns, and equipment for published results.

For BANs the separation of measurement-result from measurement-instrument may not apply [6]. The human body impacts the antenna properties: the external measurement and the local hardware are strongly coupled [6]–[8]. Orientation and placement of sensors on the body and movement of the body (both local sensor movement, and whole network movement relative to nearby objects) have all been shown to have dramatic impact on the channel [7], [8]. This is in addition to the coupling of the body and the antenna.

Models using static voxel body representations (sometimes called body phantoms) do not capture dynamic effects. Further, point-to-point measurements on the body are substantially different to point-to-point through the body [5]. In [9, Fig.33, pp.16] the shortest path distance from on-body-point to on-body-point is a poor measure of path loss, since the real path loss is a function of 60dB loss and surface-wave path length (around the torso not through it). Unfortunately, this depends upon how, where and what type of sensors are used.

In wireless sensor networks, there is a growing view that many of the underlying (MAC-layer) assumptions may be invalid [10]. Similar views may emerge in PHY for BANs.

A. Contribution of this paper

We outline a novel design based on 2.4GHz radios, which may be easily scaled to act as a real-time wearable narrowband body area network. We provide open access hardware specifications. We provide public data sets upon which we demonstrate application of our statistical approaches, and compare results of the public data sets with large (private) data set results provided in the literature.

This paper motivates large scale open access data sets of real body area network channels, to allow for comparison and verification of future 802.15.6 compliant systems.

The remainder of this paper is arranged as follows: Section II outlines previous work on (real) narrowband ISM channel models. The difficulties for existing human-worn wireless channels motivates our work of Section III. The efficacy of the testbed design is shown in Section IV, where we demonstrate reciprocity of the channel, and typical correlation and statistical results. We compare these with existing public results taken from the same hardware. Section V provides discussion and draws conclusions.

II. Previous work and modelling approaches

Work in BAN channel models has been dominated by bulk path-loss estimation, see [7], [11] for a review. Hall [12] demonstrated RSSI measurements at 2.45GHz, for a stationary subject, finding that the channel gain was essentially constant $\pm$3dB, with the variation largely due to breathing. This is in contrast to the stationary measurements of [7], which observed substantial variation. In [13], prediction from a path-loss simulator was found to under-estimate the severity of real fades from measurements – likely due to subject movement.

Cotton *et.al.* [14] used a high-gain transmit system[1] with +22dBm transmit power, clothing-mounted high-gain amplifier receivers with a continuous wave transmit, and performed various characterizations. MICAz motes were used in [16], where subjects moved from one end of a building to the other, with a sample period of approximately 4ms. Shah *et.al.* [17] used a ZigBee radio system (Mote) to evaluate the impact of on-body placement vs normal free-space sensor networks. A range reduction from 10m to 1m was found. The sampling period was approximately 10ms. These modelling works suffer from some (or all) of the following limitations [18]:

- very short time frame measurements – *e.g.* 10-40minutes
- specific movement scenarios – *e.g.* "walking" "standing"
- simple network architectures – *e.g.* single network with a star topology and a single transmit element

[1]Australian standards [15] for radiation require a maximum output for general public of 20mW continuous power

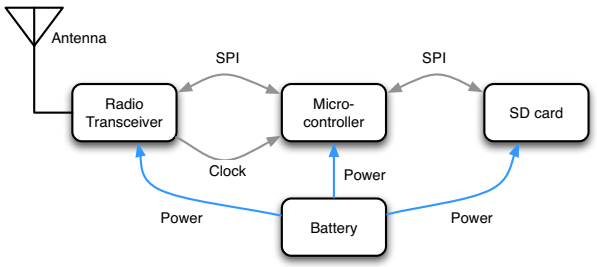

Fig. 1. Radio-Frequency testbed high level system diagram.

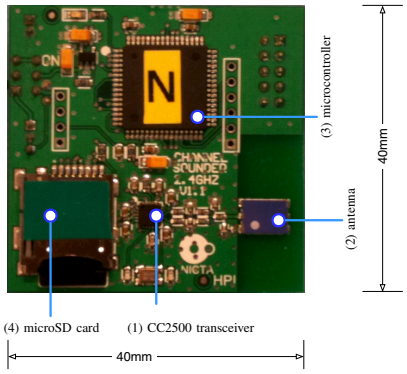

Fig. 2. The Radio-Frequency testbed with major components highlighted. Battery (diconnected) is on reverse side

- private hardware and/or private data

III. Hardware Details

The BAN channel at 2400MHz is frequency flat [19] with a time coherence on the order of 5-15ms [20]. A 5ms sample period for the narrowband channel is acceptable. The flatness of the channel implies that very low data rates (on the order of 100's of kbps) are sufficient to model the temporal response of the system. Inter-symbol interference is negligible for BANs at carrier frequencies around 2400MHz [21] – no sophisticated equaliser is required.

A. Design motivation

- large scale data collection – 15 hours at 200 samples per second gives more than 10 million sample points.
- flat antenna for proximity to body

To meet these design objectives, we chose a custom hardware solution, rather than commercial systems such as [22].

B. Functionality

The testbed is a programmable radio transceiver with non-volatile data storage, designed to be worn by test subjects for several hours. The testbed is comprised of (1) radio transceiver, (2) antenna, (3) microcontroller, (4) microSD card socket, (5) rechargeable battery.

The system is shown in Figure 1 and details are in Figure 2. The system is able to: send and receive data with other identical systems, and store and retrieve data on the microSD card. In previous works we have stored the RSSI value for each received packet.

The behaviour of the system is determined by the firmware program stored on the microcontroller's flash memory. When in operation, the system is self-contained, which allows measurements for be taken for *e.g.* sleeping, and also avoids signal-strength mis-measurement through use of long external connectors. The system possesses a small form factor and can operate continuously for over twelve hours.

C. Hardware Design and Implementation

1) Radio Transcreiver: The Texas Instruments CC2500 makes up the RF front end of the hardware platform. The CC2500 is a complete baseband modem, and communicates digital data in the form of packets with the microcontroller [23]. The System-On-Chip RF front end was chosen due to the minimal number of parts required and therefore small form factor and increased reliability. This device is specified by the manufacturer to work within the 2.4GHz ISM band, but will operate over a much wider range if programmed to do so. This capability was exploited in our experiments to perform measurements at 2.36GHz. The device was used with a nominal output power set to 0dBm.

2) Antenna: A Bluetooth surface-mount ceramic multilayer "chip" antenna was used (YAGEO CAN4311111002451K). Chip antennas possess a very small form factor and are physically robust but have a low efficiency compared to air dielectric equivalents. This antenna is likely to mimic the chip antennas used in body-mounted BANs.

A matching network was employed between the CC2500 and the antenna. This matching network also acted as a balun, and was copied from the CC2500 Reference Design [24]. The transmitted power at the antenna was measured using a Rhode and Schwartz FSH6 Spectrum Analyser, an Octane Wireless 2.4-2.5 GHz antenna with an operational efficiency of greater than 85%, and a gain of 0dBi. A total power of -9.94dBm in a measurement bandwidth of 3.84MHz was recorded in free space[2].

3) Microcontroller: The Atmel ATmega1281 (AVR core) was the microcontroller used in this design. This part was chosen for its low power consumption and large on-board flash memory (256kBytes) [25]. The microcontroller controls the sending and receiving of data from the radio, writing to the storage device (SD card), and the timing of the system.

4) SD Card: A microSD card was used to store gain measurements. MicroSD cards are the cheapest and physically smallest form of non-volatile storage available at the time of print. By using FAT formatted microSD cards, the files could be transferred to a computer using an off-the-shelf card reader.

5) Battery: A nickel metal hydride 3.6V 600mAh cordless phone battery was used to power the system (Energizer CP18NM). Lithium type batteries have superior energy density

[2]We have also matched the design against free-space D^2 path loss, and found that the receiver has similar loss – ie, a 0dBm transmit power, point-to-point link at 1m in free space records approx. -20dB, rather than 0dB.

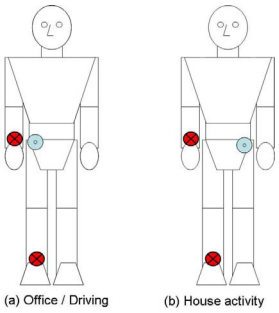

Fig. 3. Physical arrangement of sensors on a human test subject. Notations: Transmitter (⊙) and Receiver (⊗).

per mass and volume but no models were easily available in a form factor suitable for this application. The battery chosen had a form factor similar to that of the PCB used and could be conveniently mounted on the underside of the PCB.

D. Software Design and Implementation

1) Microcontroller Firmware: The firmware for the ATmega was developed in house, with the open source software project Tiny-FatFs [26] used to store files on the microSD card. The firmware was composed of several layers. The Hardware Abstraction Layer (HAL) performed low level hardware control of the device peripherals, timers, RF front end and SD card. The application layer implemented the wireless protocol and data logging.

All transceivers were enumerated, and the system used a TDMA protocol with fixed time slots to guarantee collision avoidance. Timing synchronisation was performed between devices to overcome drift between device clocks. In the case of multiple transmitters, each transmitter was operated in round-robin style, which ensured all networks avoided interference. This round-robin protocol results in a sampling frequency of $200/N$ Hz for N transmitters.

IV. Analysis of Data

We analyse (i) first order statistics (ii) second order statistics and (iii) reciprocity of the BAN channel. Channel measurements were made at 2360 MHz (near ISM band, avoiding ISM interference) and the device transmitted at 0dBm at a rate of 200 Hz (*i.e.*, one packet every 5ms). With each transmission, the receiving node recorded the Received Signal Strength Indicator (RSSI) for the packet and derived the path gain for each Tx/Rx link. The receiver sensitivity of the link is set to -100dBm, below which the packet is dropped.

Data analysis was performed for a single star topology, using [27]. Activities included routine office activity, driving a car and performing household activity. For each activity type, sensor locations on the test subject are shown in Fig. 3.

A. First Order Statistics: Distribution of Channel Gain

We obtained maximum likelihood (ML) estimates, of normalized received signal amplitude data for the public data-set, for six standard distributions often used in channel characterization and modeling, i.e the Rayleigh, Normal, Lognormal, Gamma, Weibull and Nakagami-m distributions. There are four sets of link data (transmit-to-receive): right hip to right wrist, right hip to right ankle, left hip to right wrist and left hip to right ankle. We apply two different normalization methods to find best-fitting distributions, normalizing each link to mean, and normalizing each link to median; and then concatenating to find best fitting distribution. Median path losses are given in Table I.

TABLE I
Median path gains for several links

Link	Path Gain
R. Hip→R. Wrist	-61 dB
R. Hip→L. Wrist	-62 dB

Link	Path Gain
L. Hip→R. Wrist	-75 dB
L. Hip→R. Ankle	-65.55 dB

TABLE II
Channel coherence: time before link-to-link correlations cross 0.7.

Activity	Transmitter Locations	Time Coherence τ (ms)	
		Right Wrist	Right Ankle
Office	Right Hip	1,110	955
Drive	Right Hip	755	3,820
Home	Left Hip	125	145

We find the best fitting distribution according to the negative log-likelihood criterion with ML parameter estimates, in both cases of normalizing to mean, and normalizing to median, to be a lognormal distribution with probability density function (pdf)

$$f(x|\mu,\sigma) = \frac{1}{x\sigma\sqrt{2\pi}} \exp\left\{\frac{-\left(\ln(x)-\mu\right)^2}{2\sigma^2}\right\}, \qquad (1)$$

where $\ln(\cdot)$ is the natural logarithm. When normalized to median, the relevant parameters are log-mean, $\mu = -0.0340$ and log-standard deviation $\sigma = 0.802$ for the fit to normalized channel gain. When normalized to mean $\mu = -1.02$, $\sigma = 0.870$ for the fit to channel gain. These distribution fits are consistent with previous results, e.g. [8], which suggest a lot of random multiplicative effects for dynamic measurements in an indoor office environment; hence additive in the log-domain to a Normal distribution (due to the central limit theorem).

The lognormal distribution fits, along with empirical normalized pdf data, are shown in Figure 4. Also overlayed is the best-fitting Gamma distribution, which is the next best-fitting distribution (of the six tested) according to negative log-likelihood criterion. The pdf for the Gamma distribution is

$$f(x|a,b) = \frac{1}{b^a\Gamma(a)} x^{a-1} \exp\left\{-\frac{x}{b}\right\}, \qquad (2)$$

where $\Gamma(\cdot)$ is the Gamma function. The shape parameter, $a = 1.535$, and scale parameter $b = 0.902$, with respect to the Gamma distribution fit shown in Fig. 4 with normalization to median of channel gain, and $a = 1.426$, $b = 0.374$ with normalization to mean.

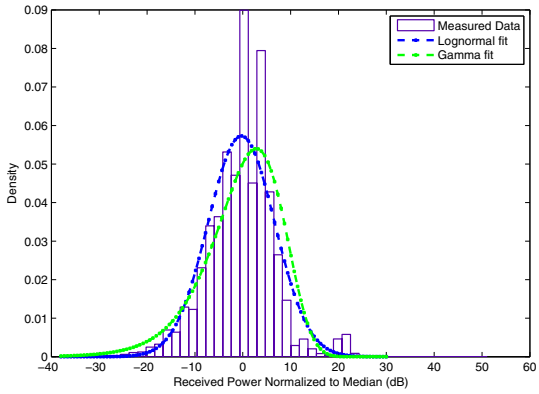

(a) Channel gain and best fit, with normalization to median

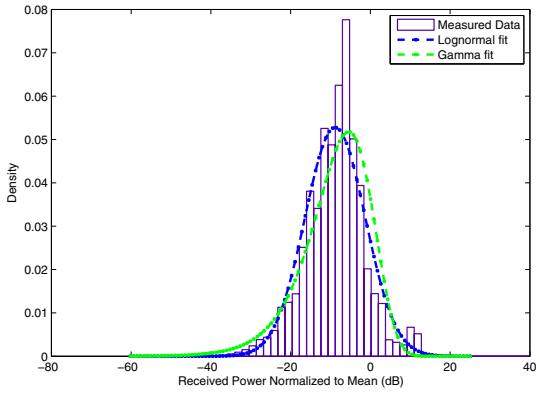

(b) Channel gain and best fit, with normalization to mean

Fig. 4. Best fits and empirical data of normalized received signal powers.

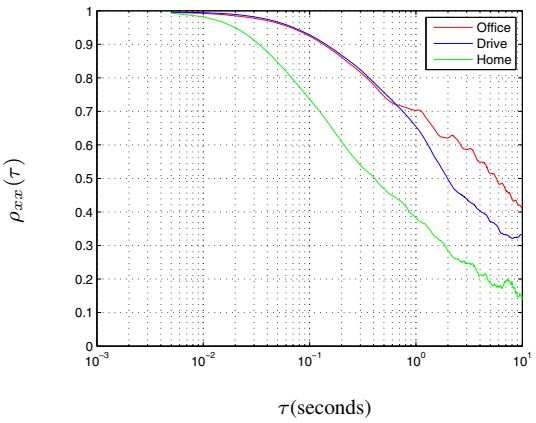

(a) Autocorrelation: Right wrist

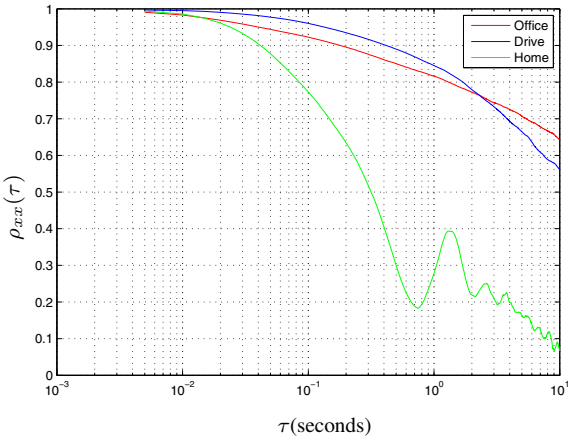

(b) Autocorrelation: Right ankle

Fig. 5. Autocorrelation for Hip → Wrist and Hip → Ankle when the subject is driving, in the office and at home.

B. Second Order Statistics:Correlation

For real discrete sampled data x_n and y_n, the normalized empirical correlation is given as:

$$\rho_{xy}(\tau) = \frac{\sum_{n=1}^{N-\tau} \{x_n - m_x\}\{y_{n+\tau} - m_y\}}{\sqrt{\sum_{n=1}^{n=N-\tau} \{x_n - m_x\}^2} \sqrt{\sum_{n=1}^{n=N-\tau} \{y_{n+\tau} - m_y\}^2}},$$

where m_x and m_y are the mean of sampled data x_n and y_n, respectively, τ is the time delay and N is the length of each measurement.

The correlation is performed over the entire data sample for lags up to one minute ($N = 12000$ samples) of data. Auto-correlation and cross-correlation for each link along with the channel coherence time is calculated. Channel coherence time is defined as the time lag for which the channel correlation coefficient remains above 0.7.

The channel coherence time is given in Table II for each Tx/Rx link. The transmitter location is changed to the left-hip six hours into the experiment when the subject is at home. Cross-correlation between the right-ankle and right-wrist was found to be negligible $(0 - 0.2)$, and is omitted from further discussion. Figures 5(a) and 5(b) show the autocorrelation graphs for the three user activities over the range of 10 seconds.

The is most coherent when subjects are in the office or driving. For office activity, the Subject is mostly sitting at the desk, and the right-wrist and right-ankle show almost identical correlation of approximately 1 second. While driving, the right-ankle depicts the largest coherence time of 3.82 seconds.

For essentially stationary activities, there is high correlation for both receivers with a slow decay rate of the correlation coefficients. When subject motion dominates, (*e.g.*at home) greater activity is reflected in smaller coherence times for right wrist and right ankle of 125ms and 145ms respectively. This is comparable to [28], [29], where the data is shown to be log-normally distributed and correlation coefficients show minimal values for motion dominant scenarios.

C. Channel Reciprocity

The measurements were taken from a left hip-mounted transmitter to a chest-mounted receiver, with a 5ms round-trip delay. We denote the forward link Hip → Chest as h_{12} and the reverse link Chest → Hip as h_{21}. The experiment was

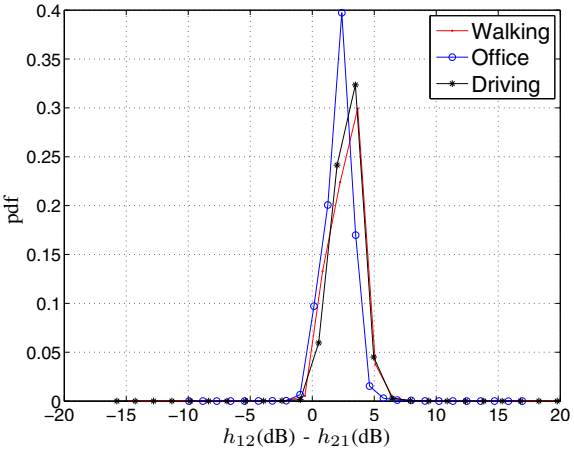

Fig. 8. Distribution of link power difference h_{12} (dB)- h_{21} (dB) for activities of walking, office and driving. Exact channel reciprocity occurs when h_{12} (dB) - h_{21} (dB) = 0 dB.

performed with two male test subjects and subject movements were annotated in 30-60 mins intervals. Fig. 6 shows the channel gains h_{12} and h_{21} for a subject (a) walking, (b) performing routine office activities and (c) driving a motor vehicle (car).

Measured channel gain profiles in the forward and reverse links almost identical in shape with a small offset in channel gain between the two links, caused due to the non-identical transceiver losses at either end of the channel. Fig. 7 depicts the scatter plots for two links and Fig. 8 depicts the distribution of link power difference

$$\text{link\_power\_diff} = h_{12} - h_{21} \text{ (dB)} \quad (3)$$

for all three activities. Exact reciprocity occurs when link_power_diff $= 0$ dB (or all markers in Fig. 7 align on the line $h_{21} = h_{12}$). The difference between the measured channel gains for forward and reverse links is negligible.

This implies that given a star network measurement (one transmitter and many receivers), we may arbitrarily reverse some of the links, to model multiple synchronous networks, or interference networks. In this way, a small number of simple star measurements may be used to generate complex network topologies.

V. Conclusion

We have outlined the design of 2.4GHz body area network radio channel modelling hardware, and provided sample data. The hardware design and the public data has been made available online from www.nicta.com.au/research/projects/human_performance_improvement/researchoutcomes/wireless. We believe the adoption of an open-access mechanism for data and measurement equipment will lead to improved reference designs for BANs.

We have shown that the public data set has similar first- and second-order characteristics to published works and have confirmed the reciprocity of the channel, thereby allowing arbitrary network configurations to be simulated with simple measurement campaigns.

Acknowledgment

The authors would like to thank the test subjects for their cooperation. The data collection was carried out under Human Ethics Protocol: *2008/254 Understanding Dynamic Radio Effects Caused by Human Motion.*

NICTA is funded by the Australian Government as represented by the Department of Broadband, Communications and the Digital Economy and the Australian Research Council through the ICT Centre of Excellence program.

References

[1] I. F. Akyildiz, Y. Sankarasubramaniam, and E. Cayirci, "Wireless sensor networks: A survey," *Computer Networks*, vol. 38, no. 4, pp. 393–422, Mar. 2002.

[2] M. D. McDonnell, A. N. Burkitt, D. B. Grayden, and H. Meffin, "The optimal number of electrodes for future cochlear implants: An information theoretic approach," in *Neuro Eng*, Melbourne, Australia, Nov. 2008.

[3] S. Abedi, G. S. Ahn, M. A. Ameen, T. Arunan *et al.*, "MAC and security baseline proposal – normative text, ID: P802.15-09-0196," IEEE submission, Mar. 2010.

[4] A. Batra, P. Bradley, C. Chaplin, M. Dawkins *et al.*, "Draft text for narrowband physical layer ID: P802.15-10-195," IEEE submission, Mar. 2010.

[5] K. Y. Yazdandoost and K. Sayrafian-Pour, "Channel model for body area network (BAN)," IEEE submission, Doc.ID: IEEE-802.15-08-0033, Nov. 2008.

[6] K. Yazdandoost, H. Sawada, S.-T. Choi, J. Takada, and R. Kohno, "Channel characterization for ban communications ID:15-07-0641," IEEE submission, 2007.

[7] L. W. Hanlen, D. Miniutti, D. B. Smith, D. Rodda, and B. Gilbert, "Co-channel interference in body area networks with indoor measurements at 2.4GHz: distance-to-interferer a poor measure of received interference power," *Springer International Journal of Wireless Information Networks*, 2010, http://www.nicta.com.au/research/research_publications/show?id=3492.

[8] D. B. Smith, L. W. Hanlen, D. Miniutti, J. A. Zhang, D. Rodda, and B. Gilbert, "Statistical characterization of the dynamic narrowband body area channel," in *Intl. Symp. App. Sci. Bio-Med. Comm. Tech.*, Aalborg, Denmark, Oct. 2008.

[9] D. B. Smith, "Electromagnetic characterisation through and around human body by simulation using SEMCAD X," NICTA, Tech. Rep. CRL-3282 http://www.nicta.com.au/research/research_publications/show?id=1504, Apr. 2008.

[10] K. Srinivasan, P. Dutta, A. Tavakoli, and P. Levis, "An empirical study of low power wireless," *ACM Trans. Sensor Net.*, 2010.

[11] A. Taparugssanagorn, A. Rabbachin, M. Hamalainen, J. Saloranta, and J. Iinatti, "A review of channel modelling for wireless body area network in wireless medical communications," in *Proc. 11th Inter. Symp. on Wireless Personal Multimedia Communications (WPMC)*, 2008.

[12] P. S. Hall, M. Ricci, and T. M. Hee, "Measurements of on-body propagation characteristics," in *IEEE International Symposium, Antennas and Propagation Society*, June 2002, pp. 310–313.

[13] K. I. Ziri-Castro, W. G. Scanlon, R. Feustle, and N. E. Evans, "Channel modelling and propagation measurements for a bodyworn 5.2 GHz terminal moving in the indoor environment," in *IEEE Int. Symp. Antennas & Propagation*, 2003, pp. 67–70.

[14] S. L. Cotton and W. G. Scanlon, "An experimental investigation into the influence of user state and environment on fading characteristics in wireless body area networks at 2.45 GHz," *IEEE Trans. Wireless Commun.*, vol. 8, no. 1, pp. 6–12, Jan. 2009.

[15] *Maximum Exposure Levels to Radiofrequency Fields - 3 kHz to 300 GHz*, ser. Radiation Protection Series. Australian Radiation Protection and Nuclear Safety Agency, Mar. 2002, no. 3.

[16] S. L. Cotton and W. G. Scanlon, "A statistical analysis of indoor multipath fading for a narrowband wireless body area network," in *IEEE Intl. Symp. Personal, Indoor and Mobile Radio Commun., PIMRC*, 2006, pp. 1–5.

[17] R. C. Shah and M. D. Yarvis, "Characteristics of on-body 802.15.4 networks," in *WiMesh*, Reston, VA, Sep. 2006, pp. 138–139.

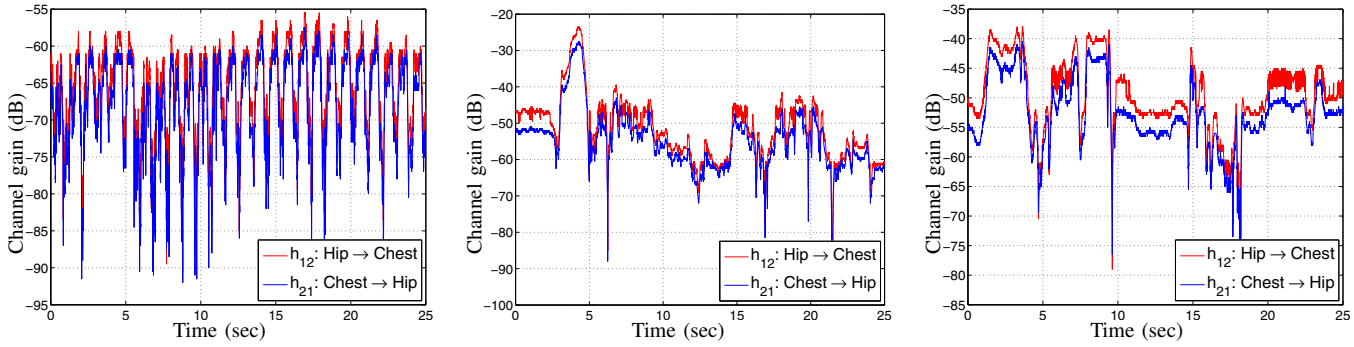

(a) Walking (b) Office (c) Driving

Fig. 6. Channel gains for links Hip → Chest (h_{12}) and Chest → Hip (h_{21}) for activities of walking, office and driving.

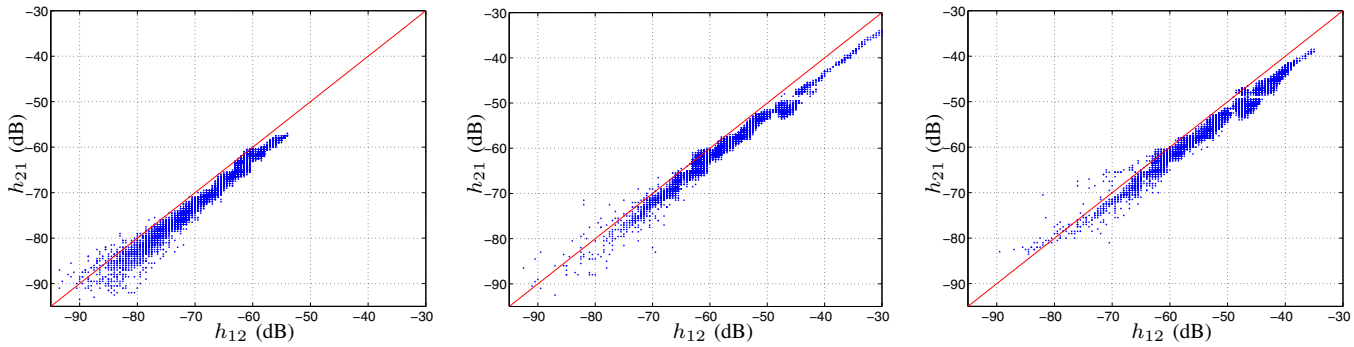

(a) Walking (b) Office (c) Driving

Fig. 7. Channel gain scatter plot h_{12} versus h_{21} for activities of walking, office and driving. Exact channel reciprocity occurs when markers align on the diagonal straight line $h_{21} = h_{12}$ shown in red.

[18] L. An, M. J. Bentum, A. Meijerink, and W. G. Scanlon, "Radio channel modeling in body area networks," in *W3 Workshop on the Pervasive Application of Wireless Technologies, Enschede, The Netherlands*, 2009, pp. 1–3.

[19] D. Miniutti, L. W. Hanlen, D. B. Smith *et al.*, "Narrowband channel characterization for body area networks ID: 802.15.08.0421," IEEE submission, Jun. 2008.

[20] J. A. Zhang, D. B. Smith, L. W. Hanlen, D. Miniutti, D. Rodda, and B. Gilbert, "Stability of narrowband dynamic body area channel," *IEEE Antennas Wireless Propagat. Lett.*, vol. 8, pp. 53–56, 2009.

[21] D. B. Smith, D. Miniutti, L. W. Hanlen, J. A. Zhang, D. Rodda, and B. Gilbert, "Power delay profiles for dynamic narrowband body area network channels IEEE P802.15-09-0187," IEEE submission, Mar. 2009.

[22] "MICAz datasheet," Strongbow www.xbow.com.

[23] Chipcon Products, from Texas Instruments, "CC2500 low-cost low-power 2.4 GHz RF transceiver," Datasheet http://focus.ti.com/docs/prod/folders/print/cc2500.html.

[24] ——, "CC2500EM 062," Desgin notes http://focus.ti.com/docs/prod/folders/print/cc2500.html.

[25] Atmel, "8 bit microcontroller with 64k/128k/256k bytes in-systems programmable flash," Datasheet www.atmel.com/atmel/acrobat/doc2466.pdf.

[26] ChaN, "Fat file system module," April 2010, http://elm-chan.org/fsw/ff/00index_e.html.

[27] L. W. Hanlen and D. Rodda, "Public dataset for BAN radio channel models," online, http://nicta.com.au/research/projects/human_performance_improvement/researchoutcomes/wireless, Mar. 2010.

[28] J. A. Zhang, L. W. Hanlen, D. Miniutti, D. Rodda, and B. Gilbert, "Interference in body area networks: Are signal-links and interference-links independent?" in *IEEE Intl. Symp. Personal, Indoor and Mobile Radio Commun., PIMRC*, Sep. 2009.

[29] V. Chaganti, D. Smith, and L. W. Hanlen, "Second order statistics for many-link body area networks," 2010, to appear.